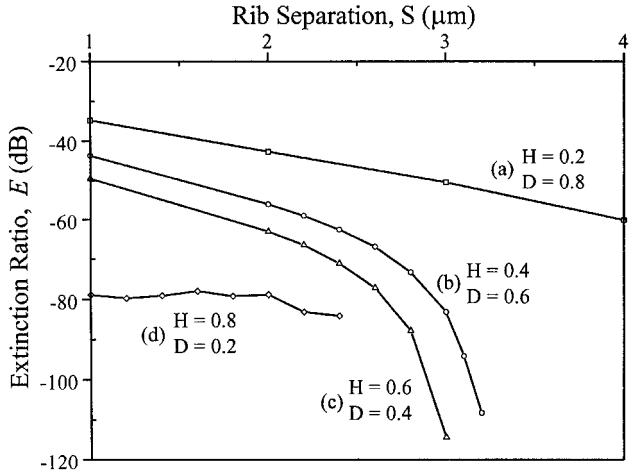

Figure 3 Extinction ratio E plotted against varying rib separation S for (a) $H = 0.2$ μm, $D = 0.8$ μm, (b) $H = 0.4$ μm, $D = 0.6$ μm, (c) $H = 0.6$ μm, $D = 0.4$ μm, and (d) $H = 0.8$ μm, $D = 0.2$ μm

crosstalk (less than -40 dB) with a coupling length that is weakly dependent on the rib separation, a moderate rib height such as the one in case (b) should be chosen. The weak dependence of the coupling length on the rib separation is to allow for a larger error margin in fabricating the rib waveguide switches.

IV. CONCLUSION

The discrete spectral index (DSI) method has provided fast and accurate calculation of the crosstalk and coupling length in optical switches which are constructed from symmetric twin-rib waveguides. An optimized rib height should be chosen such that a low enough crosstalk (less than -40 dB) is achievable with a coupling length characteristic that is weakly dependent on the separation between the ribs so that there is increased error tolerance in the fabrication of the rib waveguide switches. Although twin-rib waveguides with a very high rib height can give crosstalk levels as low as -80 dB, the coupling length is difficult to control during fabrication due to its strong dependence on the separation between the ribs.

REFERENCES

1. K. L. Chen and S. Wang, "Cross-Talk Problems in Optical Directional Couplers," *Appl. Phys. Lett.*, Vol. 44, Jan. 1984, pp. 166–168.
2. H. A. Haus and N. A. Whitaker, Jr., "Elimination of Cross Talk in Optical Directional Couplers," *Appl. Phys. Lett.*, Vol. 46, Jan. 1985, pp. 1–3.
3. J. P. Donnelly, H. A. Haus, and L. A. Molter, "Cross Power and Crosstalk in Waveguie Couplers," *J. Lightwave Technol.*, Vol. 6, Feb. 1988, pp. 257–268.
4. M. G. Daly, P. E. Jossop, and D. Yevick, "Crosstalk Reduction in Intersecting Rib Waveguides," *J. Lightwave Technol.*, Vol. 14, July 1996, pp. 1695–1698.
5. P. C. Kendall, M. S. Stern, and P. N. Robson, "Discrete Spectral Index Method for Rib Waveguide Analysis," *Opt. Quantum Electron.*, Vol. 22, 1990, pp. 555–560.
6. P. N. Robson, P. C. Kendall et al., *Rib Waveguide Theory by the Spectral Index Method*, Research Studies Press Ltd., Johy Wiley & Sons, New York, 1990.
7. S. V. Burke, "Planar Waveguide Analysis by the Spectral Index Method II: Multiple Layers, Optical Gain and Loss," *Opt. Quantum Electron.*, Vol. 26, 1994, pp. 63–77.
8. M. S. Stern, "Comparison of Spectral Index, Semi-Vectorial Finite Difference and Vector Finite Element Methods for the Modal Analysis of Semiconductor Rib Waveguide," *Int. Conf. Computation in Electromagnetics*, IEEE COnf. Publ. 350, 1991, pp. 18–21.

CCC 0895-2477/98

A BROADBAND MICROSTRIP-TO-SLOT-LINE TRANSITION

M. M. Zinieris,[1] R. Sloan,[1] and L. E. Davis[1]
[1] Department of Electrical Engineering and Electronics
UMIST
Manchester M60 1QD, England

Received 22 January 1998

ABSTRACT: *This paper presents a double slot-line–microstrip transition employing a 90° cross over them. Using radial stubs at the crossover between the transmission lines, an insertion loss of less than 1.3 dB was measured (0.65 dB per transition) over the 3–15 GHz range. The transition is simulated using a commercial electromagnetic finite-element simulator.* © 1998 John Wiley & Sons, Inc. Microwave Opt Technol Lett 18: 339–342, 1998.

Key words: *microstrip; slot line; transition*

1. INTRODUCTION

Microstripline–slot-line transitions have a number of useful applications in microwave devices including pulse inverters and a variety of hybrids [1]. Many workers have dealt with the microstrip–slot-line transition problem [2–7], reporting bandwidths from an octave [2] up to one decade in the 1–10 GHz range [7]. The simplest of these wideband transitions seems to be the one proposed by Schüppert [5] based on the 90° crossing. The wideband transitions presented by Scieck and Köhler [6] and Soltysiak and Chramiec [7] require metallized through holes and multiarm stubs at angles other than 90°, respectively. In this paper, we examine a transition similar to that proposed in [5], but using radial stub instead of a circular one. The geometry of the stubs alleviates the problem of overlapping of the line shapes between the microstrip and slot-line tuning stubs. Such overlapping generally disturbs the effectiveness of the microstrip ground plane. In addition, radial stubs exhibit a broader bandwidth than straight ones.

2. THEORY

Consider the transition of Figure 1. The microstrip open circuit radial stub should appear as a short circuit, and the slot-line short circuit radial stub should appear as an open circuit at the crossing reference plane. The equivalent circuit of the above transition with the input on the microstrip line [1] is shown in Figure 2.

L_{os} is the inductance of the shorted slot line. C_{oc} is the capacitance of the open microstrip. Z_{os}, Z_{om} are the slot-line and microstrip characteristic impedances, respectively. θ_s, θ_m are the electrical lengths (quarter wavelength at center frequency) of the extended portions (stubs) of the slot-line and microstrip, respectively. n is the transformer ratio.

Expressions for the above parameters can readily be found in the literature [1].

Using the equivalent circuit and transforming all of the circuit's components to the microstrip side, we obtain the

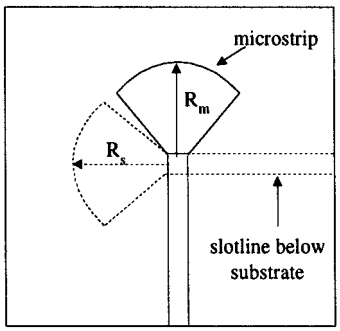

Figure 1 Microstrip–slot-line transition with radial stubs

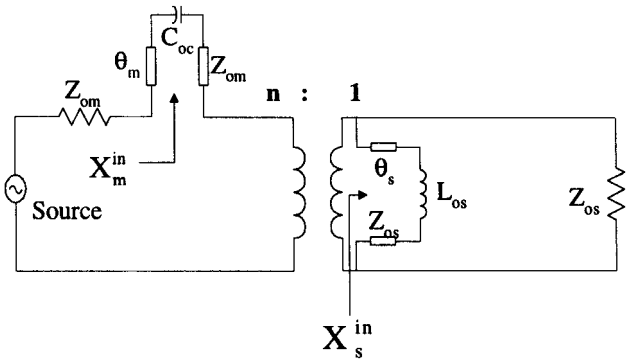

Figure 2 Equivalent circuit for the transition

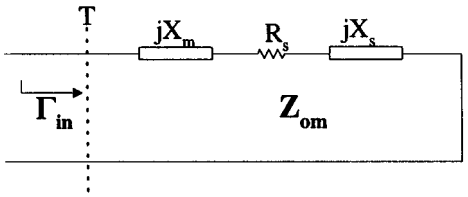

Figure 3 Equivalent circuit after transformation

equivalent circuit of Figure 3 where

$$R_s = \frac{n^2 Z_{os} X_s^{in}}{Z_{os}^2 + X_s^{in}} \tag{1}$$

$$X_s = \frac{n Z_{os} X_s^{in}}{Z_{os}^2 + X_s^{in}} \tag{2}$$

$$X_m = X_m^{in} \text{ (see Fig. 2).}$$

The input reflection coefficient Γ_{in} is therefore given by

$$\Gamma_{in} = \frac{R_s - Z_{om} + j(X_m + X_s)}{R_s + Z_{om} + j(X_m + X_s)}. \tag{3}$$

X_m can be computed by the expression proposed by Atwater [8] and standard transmission line equations. However, no model is available for the reactance presented by the slot-line stub and, consequently, the input reflection coefficient cannot be computed. However, the following arguments can help us circumvent this problem. It was shown in [9] that for broadband operation, the physical length of a *circular* stub should be approximately $l \approx 1.5d$ (where d is the diameter). If a similar approximation is adopted for the radial stub, a similar argument should hold true due to its geometric proximity with the former (but with the diameter replaced by the radius). At a center frequency f_0, the slot-line radial stub is equivalent (electrically) to a quarter-wavelength straight stub. It therefore follows that the radius of the radial slot-line stub should be $(\lambda_s/4) \approx 1.5r_s$, that is, $r_s \approx (\lambda_s/6)$. It is recognized that the slot-line length is responsible for a ripple in the transmission coefficient in a way yet to be quantified. An electromagnetic simulator by Hewlett-Packard (HFSS™ version 1) was used to establish the optimum slot-line length as well as to check the rather simplistic procedure leading to the radial stub radius.

3. DESIGN AND EXPERIMENTAL VERIFICATION

The simplest way to measure the frequency response of this transition is to measure the transmission coefficient of two transistions in cascade. This facilitates easier fabrication and calibration. The double transition was designed on a 0.635 mm thick RT/Duroid™ 6010 ($\epsilon_r \approx 10$) substrate. The center frequency was set at $f_0 = 10$ GHz. The characteristic impedances of the microstrip and slot line were nominally $Z_{om} = 50\ \Omega$ and $Z_{os} = 50\ \Omega$. The slot-line impedance was

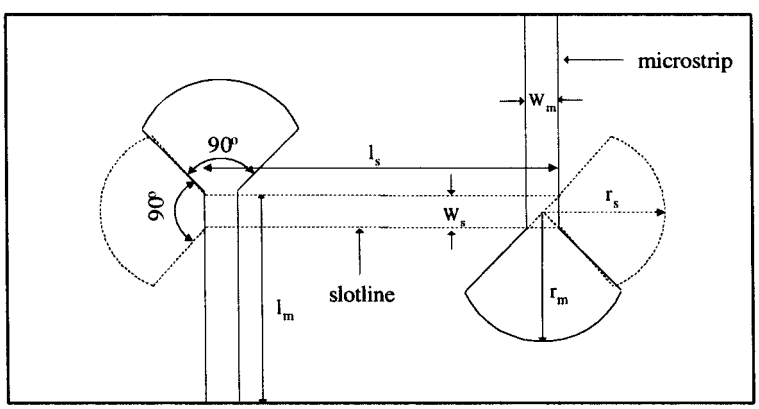

Figure 4 Dimensions of the double transition

selected as 72 Ω as a compromise between the narrow slot width required to obtain $Z_{os} = 50$ Ω and the limitations of the available fabrication technique. These values were allowed to vary in the optimization procedure in order to reduce the predicted insertion loss. After the optimization procedure (using HFSS), the dimensions shown in Figure 4 were established, where $w_s = 0.156$ mm, $w_m = 0.66$ mm, $l_s = 5.25$ mm, $l_m = 5$ mm, $r_s = 2.6$ mm, and $r_m = 2.4$ mm.

The slot-line wavelength at 10 GHz is 15 mm, and according to the simple procedure given in the preceding section, the slot-line radial stub radius should be $r_s = 2.5$ mm. The optimized radius was found to be 2.4 mm, a difference of 4%. It seems, therefore, that this simple procedure can give reasonable initial values from which a CAD procedure can be utilized in the circuit design.

The transition was fabricated, and the structure was enclosed in a metallic shield to prevent excessive radiation losses, and the following dimensions were recorded: $w_s = 0.17$ mm, $w_m = 0.74$ mm, $l_m = 5.1$ mm, $l_s = 5.2$ mm, $r_s = 2.8$ mm, and $r_m = 2.7$ mm.

Coaxial connectors were soldered on the input and output microstrip lines. The transmission coefficient was measured with an HP 8510 vector network analyzer. Figure 5 shows the measured and simulated response (lossless lines and dielectric were assumed) of the transition. Figure 6 shows the measured return loss of the circuit.

As can be seen, there is good agreement between simulation and experiment in the passband (3–15 GHz) where the shape of the frequency response is preserved. The measured response has an insertion loss below 1.3 dB from 3.2 to 15.5 GHz. Since this corresponds to the double transition, the maximum insertion loss power transition is 0.65 dB. It is observed that the ripple in the passband is appreciable. This can be attributed to the detuning effect brought about by the overetching in the fabricated circuit. The substantial return loss of the transition can also be attributed to the same effect. A circuit incorporating the dimensions of the fabricated circuit was simulated in HFSS, and the ripple effect was noticeable. By removing the top and bottom covers of the metallic enclosure, the radiation losses were observed. Between 3–7 GHz, radiation contributed approximately another 0.4–0.5 dB losses, whereas between 8–16 GHz, there was approximately 1–1.2 dB extra loss. This highlights the need for shielding, especially at high frequencies. Of course, one has to be careful with the enclosure dimensions so as not to excite resonances.

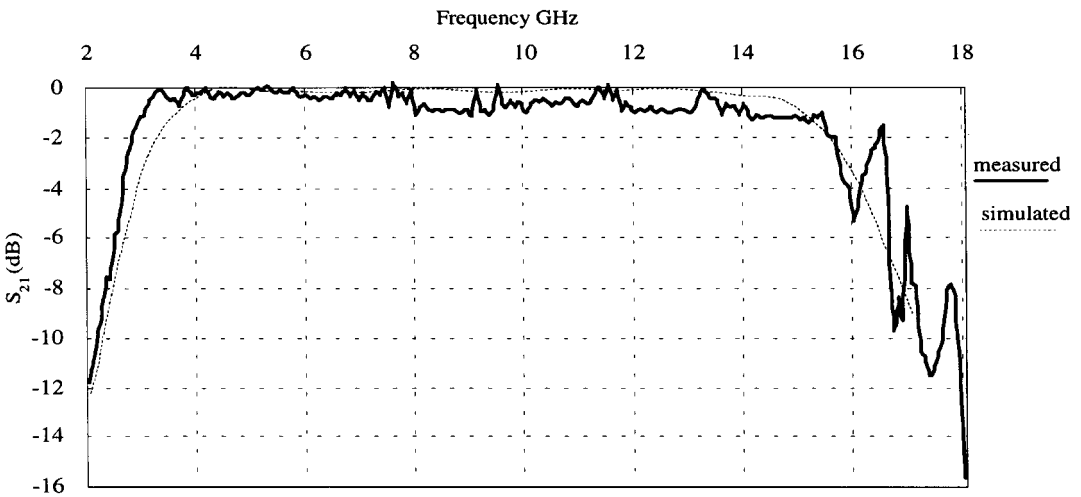

Figure 5 Measured and simulated transmission coefficient of double transition

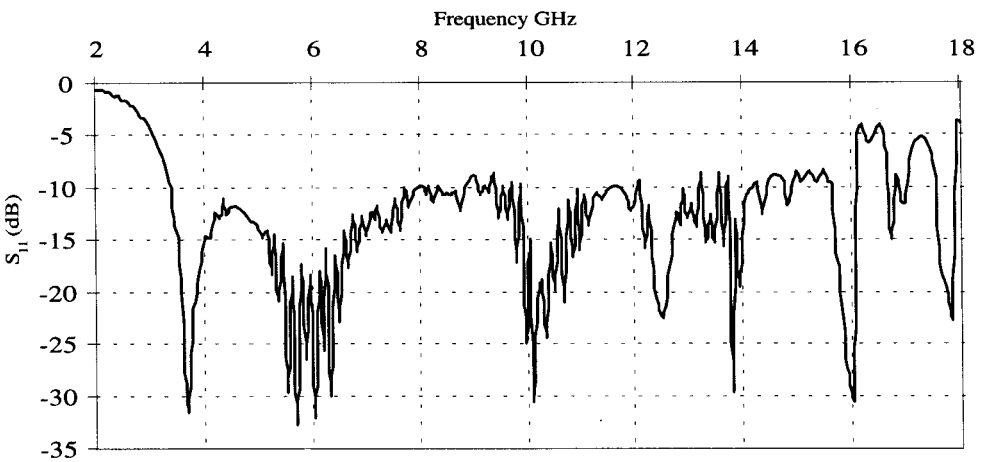

Figure 6 Measured return loss of the transition

4. CONCLUSIONS

The suitability of radial microstrip and slot-line stubs for the realization of broadband microstrip-to-slot-line transitions has been demonstrated. A simple procedure has been utilized to estimate the length of the slot-line radial stub for which an analytic model is still lacking. With an insertion loss of less than 0.65 dB per transition over the 3–15 GHz band, the agreement between the measured and predicted performance is encouraging. It is expected that refinements in the design will yield improved performance.

ACKNOWLEDGMENT

One of the authors (M. M. Zinieris) wishes to thank the Overseas Research Students Awards Scheme (ORS) for its financial support.

REFERENCES

1. K. C. Gupta, R. Garg, and I. J. Bahl, *Microstrip Lines and Slotlines*, Artech House, Norwood, MA, 1979.
2. J. B. Knorr, "Slotline Transitions," *IEEE Trans. Microwave Theory Tech.*, Vol. MTT-22, 1974, pp. 548–554.
3. A. Radmanesh and W. A. Bradford, "Generalised Microstrip-Slotline Transitions: Theory and Simulation Vs Experiment," *Microwave J.*, June 1993.
4. A. Podcameni and M. L. Coimbra, "Slotline-Microstrip Transition on Iso/anisotropic Substrate: A More Accurate Design," *Electron. Lett.*, Vol. 16, No. 20, 1980, pp. 780–781.
5. B. Schüppert, "Microstrip-Slotline Transitions: Modeling and Experimental Investigation," *IEEE Trans. Microwave Theory Tech.*, Vol. 36, 1988, pp. 1272–1282.
6. B. Scieck and J. Köhler, "An Improved Microstrip to Microslot Transition," *IEEE Trans. Microwave Theory Tech.*, Vol. MTT-24, 1976, pp. 231–233.
7. P. Soltysiak and J. Chramiec, "Design of Broadband from Microstrip to Slotline," *Electron. Lett.*, Vol. 30, No. 4, 1994, pp. 328–329.
8. A. H. Atwater, "The Design of the Radial Line Stub: A Useful Microstrip Circuit Element," *Microwave J.*, Vol. 28, 1985, pp. 149–156.
9. B. Schüppert, "Analysis and Design of Microwave Balanced Mixer," *IEEE Trans. Microwave Theory Tech.*, Vol. MTT-34, 1986, pp. 120–126.

CCC 0895-2477/98

ON THE CONSTITUTIVE PARAMETERS OF A CHIROFERRITE COMPOSITE MEDIUM

Werner S. Weiglhofer,[1] Akhlesh Lakhtakia,[2] and Bernhard Michel[3]

[1] Department of Mathematics
University of Glasgow
Glasgow G12 8QW, Scotland

[2] CATMAS — Computational & Theoretical Materials Sciences Group
Department of Engineering Science and Mechanics
Pennsylvania State University
University Park, Pennsylvania 16802-1401

[3] Astrophysikalisches Institut und Universitäts-Sternwarte
Universität Jena
D-07745 Jena, Germany

Received 23 January 1998

ABSTRACT: *The chiroferrite medium is conceptualized as a homogenized composite medium (HCM) comprising a magnetically biased ferrite and an isotropic chiral medium as its components. Numerical results are presented which show unambiguously that the HCM is fully bianisotropic with all four constitutive dyadics endowed with a gyrotropic structure. The magnetoelectric response properties depend critically on the chirality parameter and the volume fraction of its isotropic chiral component.* © 1998 John Wiley & Sons, Inc. Microwave Opt Technol Lett 18: 342–345, 1998.

Key words: *homogenized composites; chirality; ferrites; Faraday chiral media; constitutive relations; bianisotropic media*

1. INTRODUCTION

The last decade has produced a vast amount of predominantly theoretical investigations into the electromagnetics of complex linear media [1–3]. The most general of these are the so-called *bianisotropic* media that are characterized through, at most, 35 constitutive parameters in the frequency domain. The ultimate aim of all complex media research is the technological exploitation of novel electromagnetic response properties and phenomena, exhibited by new complex media, in electronic and optical devices.

Numerical studies—leading subsequently to experimental research and device development—must therefore span a vast parameter space to identify novel phenomena. Infeasible and unrealistic values of constitutive parameters must be avoided, particularly when working with artificial complex media. The aim of this communication is to report a short parametric study on the constitutive properties of chiroferrites—conceived as random dispersions of electrically small, isotropic chiral inclusions immersed in magnetically biased ferrite media [4, 5].

Chiroferrites and chiroplasmas (chiral inclusions embedded in magnetically biased plasmas) are the two examples of *Faraday chiral media* [4]. Their frequency-domain constitutive relations were developed casually in [4]. A recent investigation [6] adopted the more realistic approach of visualizing a Faraday chiral medium as a homogenized composite medium (HCM), demonstrating that the constitutive relations of any Faraday chiral medium can be derived from the constitutive parameters of its component media. Indeed, the constitutive relations given in [4] were found to be ambiguous as well as oversimplified. With the provision of the correct constitutive relations [6] and electromagnetic field representations [7, 8], the door has now opened to more realistic wave propagation and scattering research with Faraday chiral media.

2. THEORETICAL PRELIMINARIES

Let us homogenize a chiroferrite composite medium, which has two component media. The first is a magnetically biased ferrite described by the frequency-domain constitutive relations[1] [9]

$$\underline{D}(\underline{x}) = \epsilon_0 \epsilon^f \underline{E}(\underline{x}) \tag{1}$$

$$\underline{B}(\underline{x}) = \mu_0 \left[\mu^f \underline{\underline{I}} - i\mu_g^f \underline{u} \times \underline{\underline{I}} + (\mu_u^f - \mu^f) \underline{u}\underline{u} \right] \cdot \underline{H}(\underline{x}). \tag{2}$$

Here, ϵ_0 is the permittivity and μ_0 is the permeability of free space (i.e., vacuum); μ^f, μ_g^f, μ_u^f are relative permeability scalars, and ϵ^f is the relative permittivity scalar; the unit vector $\underline{u}$ is parallel to the quasimagnetostatic biasing field of the ferrite; while $\underline{\underline{I}}$ is the unit dyadic. The second component

[1] All frequency-domain field vectors and constitutive parameters depend on the circular frequency ω. Vectors are underlined once and dyadics twice, while $\cdot$ symbolizes a dot product.